Towards a bio-inspired acoustic sensor: *Achroia grisella*'s ear

Lara Díaz-García*, Student Member, IEEE, Andrew Reid, Joseph Jackson-Camargo, James F.C. Windmill, Senior Member, IEEE

***Abstract*— Gathering insight from nature to develop original solutions for engineering problems is known as bio-inspiration. The examples found in nature are often efficient and beautifully simple. For the particular issue of directional acoustic sensing at small scales, insects provide a myriad of clever adaptations to achieve hearing despite their small body size. *Achroia grisella* is a nocturnal moth capable of directional hearing of wavelengths significantly longer than its inter-tympanic distance. Previous studies have shown that directionality for this moth is monoaural and exclusively relies on the shape of the eardrum itself. The work developed a computer model that behaves similarly to the moth's ear, which is then 3D printed. The model starts from a simplified circular membrane and progresses until it reflects the moth's tympanum more closely. The approach followed consists of four steps: considering analytical equations, virtually simulating the model, manufacturing and performing experimental measurements, and finally comparing the outcomes of each. Equations are produced for the simplest geometries, and COMSOL Multiphysics is used for the simulations. The samples are manufactured via 3D printing and excited with a vibrating piezoelectric chip and a speaker while being measured with a 3D Laser Doppler Vibrometer to determine their frequency and directional responses.**

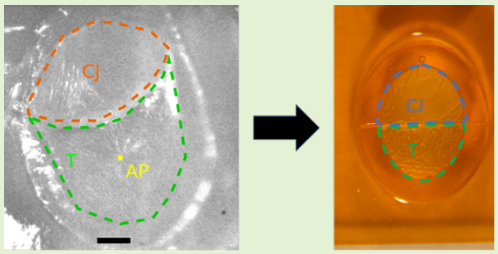

***Index Terms*—3D printing, Achroia grisella, acoustic sensor, bio-inspiration, insect hearing**

I. Introduction

HEARING is one of the ways in which animals interact with their surrounding environment. A few examples of useful applications of hearing in animals are escaping a predator, pursuing prey, communicating with conspecifics, or attracting a potential mate. In most of these cases, besides the detection of sound itself, it is particularly crucial to know the location of the sound source, hence why directional hearing is desirable for animals [1].

Hearing is commonly found in vertebrates, and intuitively identified in mammals, where we think of a pair of small flesh appendixes, the ears, that precede a subsequent pair of tympana, or eardrums. However, a hearing sense might not be as identifiable if we look at other animal classes, like arthropods, for which the hearing tools can be found all over the body and do not resemble human ears at all.

Except for mantids, animals that hear show bilateral symmetry, meaning there is an ear on each half of their bodies. Bigger animals use their two ears, separated by a certain distance, to compare the intensity, time of arrival and phase of incoming sound, locating the provenance of sound and consequently achieving directional hearing. On the other hand, smaller animals with hearing have an inter-ear distance that is not long enough for their brains to process any of these calculations, having to resort to other mechanisms instead.

Within arthropods we find the *Insecta* class, generally characterized by a small body size. Some insects have developed clever adaptations to overcome their size and perform directional hearing of sounds with wavelengths of the same scale as their body sizes. *Ormia ochracea*, for example, is a fly with tympana interconnected by a stiff tissue bridge, making the whole system move in a complex way. This grants the fly a precision of 2° when landing on their hosts, whose calls they listen for [2]–[5]. Other insects, like grasshoppers [6] and field crickets [7], have multiple openings to the outside in their tracheal systems, allowing sound to arrive to both sides of their tympana with different times and amplifications.

Lepidoptera are an order of insects composed of what are commonly called butterflies and moths. The latter, being mostly nocturnal, are predominantly predated by bats, which use echolocation for hunting. Therefore, it is believed that many moths have developed hearing in the ultrasonic range in order to anticipate the presence of hunting bats by their calls [8]. What is not so common is for moths to use their hearing sense for intraspecific communication [9].

Achroia grisella is a moth from the *Pyraloidea* superfamily. It is one of the many species that uses hearing for detecting bats. But *Achroia* are quite unique in that they use ultrasonic calling in their mating process, instead of just pheromones. The males fan their wings while remaining still [10], which produces a train of clicks (main content of the signal of 100 kHz [11]). The

Submitted for review on May 6th 2022.

All authors are affiliated with the Centre for Ultrasonic Engineering, University of Strathclyde, Glasgow, United Kingdom (e-mail corresponding author: lara.diaz-garcia@strath.ac.uk).

An earlier version of this paper was presented at the IEEE Sensors 2021 conference and was published in its Proceedings: https://ieeexplore.ieee.org/document/9639528.

females, upon listening to the signal, make their way to the males after some zigzagging.

These moths have just four auditory neurons per tympanum, and they are not capable of frequency discrimination. The way female moths differentiate a bat call from a male moth call, eliciting an evasive or positive behavior respectively, is thus believed to be time-encoded [12]. *Achroia*'s usual size is about 13 mm, which means their tympana are separated by less than 600 μm on average. This inter-ear distance is insufficient to discern any phase, intensity, or time of arrival difference for a signal of 100 kHz, which has a corresponding wavelength of 3.4 mm.

X-ray scans of moth specimens have discarded the suggestion of any existing connection between the tympana or spiracles in the body, ruling out systems like those previously mentioned. Diffraction around the insect's abdominal section cannot account for a sufficient intensity difference either [13]. Moreover, experiments where female moths had one tympanum pierced showed that they were still able to find the calling males, albeit with more difficulty [14]. For all these reasons, it is believed that directionality in *Achroia grisella* is monoaural and exclusively dependent on tympanum morphology.

II. Methodology

The working hypothesis is, therefore, that the moth's tympanum geometry confers them with a certain extent of directionality. To test it, we have developed an approach where a simple model is proposed and examined analytically, in simulation, and with real 3D printed samples measured with Laser Doppler Vibrometry. The three are then compared against each other. The model is progressively revised to improve its complexity and its resemblance to the real moth tympanum.

Before considering the model, what the moth's actual tympanum looks and behaves like was explored. *Achroia*'s tympana are approximately elliptical and divided in two distinct sections of different thicknesses. The thicker part is called *conjunctivum* and the thinner part receives the name of *tympanum proper* or simply tympanic membrane. The *scolopidium*, a cluster of four auditory neurons, is attached directly to the latter, roughly in the center of the membrane (Fig. 1).

Under exposure to a 100 kHz signal, the tympanum moves in a complex, non-drum-like pattern, with the entirety of the surface vibrating and showing local maxima and minima. The main peak appears close to, but not exactly on, the neuron attachment point. Around it we see a half ring of lower-amplitude peaks. Lastly, a broader bump of low amplitude is seen on the thicker part. They are all slightly out of phase with each other [16].

A. Analytical Approach

In the first place, to find an analytical solution, the equations of motion that describe the system are observed. Transverse vibrations on a plate, which are ruled by different equations than membranes, were considered. The reason for considering a plate and not a membrane is because bending stiffness is not negligible. The plate equation is a fourth-degree differential one:

$$\nabla^2(\nabla^2 W) + \frac{1}{c^2}\cdot\frac{\delta^2 W}{\delta t^2} = 0 \quad (1)$$

Where the terms are $\nabla^2\nabla^2 = \nabla^4$, known as the biharmonic operator; $W = W(x, y, t)$, the function that describes displacement; and c, the velocity of the wave in the medium, itself defined as:

$$c = \sqrt{\frac{E \cdot h^2}{12 \cdot \rho \cdot (1 - \nu^2)}} \quad (2)$$

The physical characteristics, Young's modulus (E), mass volume density (ρ) and Poisson's ratio (ν), are taken as 1 GPa, 1180 kg/m^3 and 0.35 respectively. The particular values of these parameters for *Achroia grisella* are not known but are chosen here using the literature regarding insect cuticle. Young's modulus is taken towards the lower end of the spectrum of values for sclerotized cuticle, and Poisson's ratio is approximately in the middle of the range [15]. The thickness of the plate (h) will be measured directly on our samples or taken from the literature as needed [16].

To find the solutions, a periodical time dependence of the function is assumed. The boundary conditions of the problem, namely the shape and nature of the perimeter, are also considered. In this case the edge is clamped. As for the shape, the problem starts from an extreme simplification, a circular plate, and progressively increases complexity.

For the first case considered, a clamped circular plate, the solutions are easily obtained because the problem is a well-known one. Polar coordinates are used to suit the nature of the problem, and its resolution involves Bessel functions.

The next step is considering a clamped elliptical plate. The resolution becomes significantly more complicated as there is a need to use elliptical coordinates and Mathieu functions. The elliptical plates' resonance frequencies will be related to the eigenvalues obtained from the solution of the transversal wave equation in the following way:

$$f_{m,n} = \frac{2 \cdot q_{m,n} \cdot c}{\pi \cdot (a^2 - b^2)}, m = 0,1,2 \ldots, n = 1,2,3 \ldots \quad (3)$$

Where $f_{m,n}$ are the resonance frequencies, in turn dependent on the eigenvalues $q_{m,n}$, c is the velocity of the wave in the medium, and a and b are the major and minor semi-axes of the ellipse respectively.

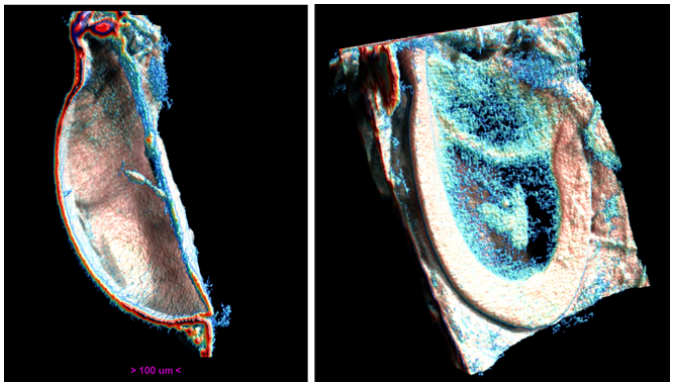

Fig. 1. Voxel reconstruction of the *Achroia grisella* tympanum from X-ray microtomography. (Left) Lateral view cross section along the major axis showing the tympanal cavity and the *scolopidium*. (Right) Front view of the tympanum showing the neuron attachment point and border between upper and lower membranes [17].

B. Simulation Approach

The simulation was carried out using the Finite Element Modelling (FEM) software COMSOL Multiphysics®. A Shell interface, from the Structural Mechanics module, is chosen for the tympanum. This interface is appropriate for considering a thin structure with considerable bending stiffness. For the resonant frequencies of the structure, a preset Eigenfrequency study is used.

For the directional response, a more general Frequency study is used. The stimulus used is in the shape of a spherical wave radiation, with an incident pressure field of 1 Pa. Two angles are set to characterize the provenance of the acoustic stimulus: polar and azimuthal. The azimuthal angle is fixed to 80º to suit our setup. A sweep of 360º over the polar angle is set, in intervals of 10º, to produce the directivity polar plots.

C. 3D Printing

3D printing was done using the digital light projection (DLP) technique. DLP has a layer-by-layer approach, creating a 2D pixel array of a slice of the design that selectively exposes the photosensitive resin to UV light, solidifying it. A printed layer will normally then fuse to the previously printed layer, however in the case of suspended regions or overhangs the layer thickness will be determined by the UV light exposure [18].

Structures were 3D printed with two different printers and materials. The structures used to initially determine the frequency responses were produced with an Original Prusa SL1 3D printer, which employs an LCD photomask to selectively pattern each material layer, and a commercial resin from the same manufacturer. The resin is Orange Tough, and it is modelled after Acrylonitrile-butadiene-styrene. The properties of the resin are obtained from the literature as a Poisson's ratio of 0.35 and volumetric mass density of 1180 kg/m^3 [19]. Young's modulus was measured in the printed samples using a 3D printed cantilever and beam theory.

The second 3D printer used was an Asiga Pico HD 3D printer and the resin chosen is a custom one composed of a base monomer, a photoinitiator, and a photo absorber. These are, respectively, Polyethylene glycol diacrylate (PEGDA) Mn 250, Phenylbis(2,4,6-trimethylbenzoyl)phosphine oxide at 0.5% weight percent, and Sudan I at 0.2% weight percent, all purchased from Merck Life Sciences and used without further modification. The resin is mixed in an ultrasonic bath (Decon FS250) for 20 minutes before use to ensure even distribution. From the literature, the Poisson's ratio and mass density of the resin are taken to be 0.32 and 1183 kg/m^3 respectively [20]. A value for Young's modulus of 52.9 MPa is also provided, but the 3D printed cantilever method, as well as compression testing, was used to determine it in these samples.

The reason for switching printing machines and moving to a custom resin was to achieve a lower Young's modulus, in turn producing lower resonant frequencies that can be excited through sound more comfortably with a common speaker for the directionality measurements. The size of the vibrating plates was increased slightly for the same reason. The aim was to produce the first three resonance frequencies under 20 kHz, reflecting the human hearing range.

The Orange Tough circular plates produced have a diameter of 1.5 mm, and the elliptical ones have major and minor axes of 2.1 mm and 1.5 mm respectively. The printed samples were examined by means of X-ray Computer Tomography using a Bruker Skyscan 1172 with SHT 11-megapixel camera and Mamamatsu 80 kV (100 milliamps) source to determine their thickness. The images generated were 1332 x 2000 pixels with a resolution of 4.98 µm per pixel. The images were collected, and a volumetric reconstruction of the sample generated by Bruker's CTvol software. The images produced are based on the level of attenuation through the sample, which is dependent on the thickness of the material and its absorption coefficient and is notably less near an object's extremities. The thickness measured is therefore dependent upon this manual thresholding. The thickness of the Orange tough samples is found to be 162 µm for single layers and 270 µm for the thicker multi-layer regions. For the custom resin, the plate has major and minor axes of 5.36 mm and 4 mm respectively. The thicknesses were examined in the same fashion and determined to be 122 µm for the single layer half and 400 µm for the thick multi-layer half. It must be noted that 3D printing of small devices is not straightforward, with residual stress gradients affecting the result significantly. Repeatability and accuracy can be difficult to achieve [21]–[24].

D. Laser Doppler Vibrometry

The printed structures were examined using 3D laser Doppler Vibrometry (3D LDV). The instrument used is an MSA-100-3D scanning head (Polytec, Waldbrom, Germany). The amplitude resolution is sub-picometer both for in-plane and out-of-plane movements, according to the manufacturer. Measurements taken in the LDV are complex averaged over 25 samples. The structures are stimulated first with a displacement piezo chip (75 V, 2.8 µm, Thorlabs, Newton, New Jersey), with wideband periodic burst signals. This allows examination of the frequency response recorded by the LDV. The resonances can be identified looking at out-of-plane vibrations and compared with the eigenfrequencies obtained from simulation, readjusted to the new parameters that match those of the 3D printed structures.

Once the resonant frequencies are found, the 3D printed plates are excited with a new setup (as seen in Fig. 2) to get the directionality measurements. Stimulation was with a Labo LB-PS1401D speaker (frequency response of 80 Hz to 20 kHz, maximum output power of 60W, sensitivity of 88 dB). The speaker was placed in an 80º angle so the normal of the speaker

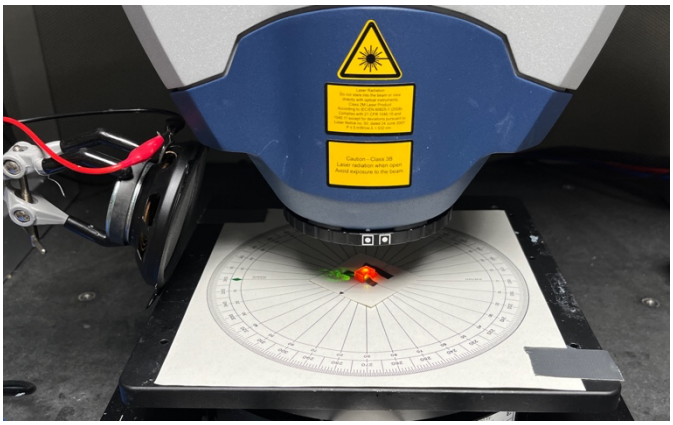

Fig. 2. Experimental setup of the directivity measurements showing the LDV, speaker, and sample being measured.

surface is not parallel to the ground. The setup is placed inside an acoustic booth and is not perfectly isolated. There is also a computer and some equipment within the booth, which may cause reflections.

The signals used consist of a series of sine tones at the resonant frequencies and the displacement at the middle point of the thin section recorded at different angles. The sample is rotated in increments of 10° and the displacement is measured at the middle point of the thin half of the two-thickness sample. The experimental data are plotted using MATLAB. The direction taken for the polar plot is that on the same plane as the plate and aligned with the major axis, with the thick half being the front and corresponding to 0°. This corresponds to where the head of the moth would point to, as can be seen in Fig. 3.

III. Results

A. Young's Modulus

Two methods are used to determine the Young's modulus of the 3D printed resins. The first one uses a cantilever in the 3D print to measure the Young's modulus of the material from beam theory by observing the resonant frequencies in the LDV [25]. Young's modulus (E) can be obtained from the following equation:

$$E = \frac{48 \cdot \pi^2 \cdot \rho \cdot f_n^2 \cdot L^4}{\lambda_n^4 \cdot h^2}, n = 1,2,3 \ldots \quad (4)$$

The parameters being mass volume density (ρ), the eigenfrequencies (f_n), the length of the beam (L), the eigenvalues (λ_n) and the thickness (h). With all other values being known, the Young's moduli thus obtained are 1.327 GPa for the Orange Tough samples and 45.38 MPa for the custom resin samples.

The custom resin sample was also tested via compression test (Instron testing). The modulus is obtained from the linear part of the stress-strain curves, resulting in a value of approximately 53 MPa, which is within 15% of the results obtained with the cantilever method for the same material.

B. Frequency Response

The results obtained from evaluating the equations in MATLAB and an eigenfrequency study run in COMSOL with the same parameters are compared. For the circular plate, the diameter considered is of 500 μm and the thickness is 5 μm. These values are of the same scale as the moth's actual tympana [10]. The frequencies provided by COMSOL are within 1% of the analytical eigenfrequencies.

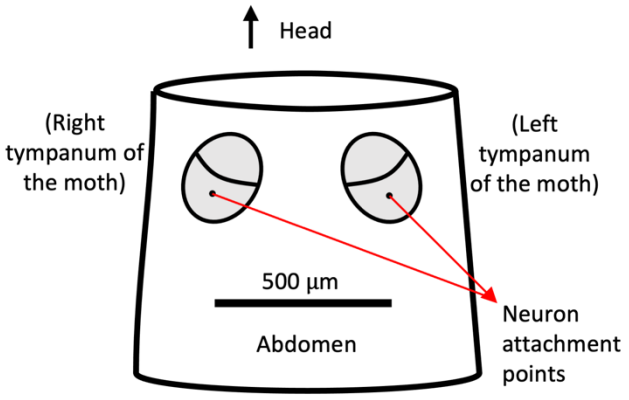

Fig. 3. Illustration of the ventral side of the first abdominal segment of *A. grisella* showing the general shape and position of the two tympana [13].

For the elliptical plate, the dimensions used are 670 μm for the major axis and 500 μm for the minor axis. The thickness considered is, again, 5 μm. Changing the geometry of the simulation to fit the new boundary conditions, the eigenfrequency study is run again, this time returning values within 7% of the frequencies predicted by the equations. It is worth noting that the vibrating patterns are still far from what is observed in the moth's tympanum for these two simple geometries. From this point onwards the equations are not considered, as they are no longer helpful in dealing with the more complex morphologies. Instead, the frequency responses of the COMSOL simulation are compared with those of the structures printed in Orange Tough. Regardless, the good agreement between COMSOL and the equations in the two previous cases is a reassurance of the validity of the eigenfrequencies predicted by COMSOL.

The next model considered includes two sections of different thicknesses, to reflect the two regions (thick and thin) of the moth's tympanum. The outline is, again, elliptical in shape. The circular, elliptical, and two-thickness elliptical plates printed with Orange Tough are examined in the LDV and the maxima of the frequency response are identified. The first few frequencies are found and compared with the COMSOL simulation, with parameters altered to match the physical properties of the printed plates. The results can be seen in Table 1. These are in good agreement with each other, as well as the mode shapes being recognizable in the LDV scans. The 3D printing is thus successful, and the structures behave as expected from the simulations.

Table 1: Frequencies from Orange Tough 3D printed plates and COMSOL simulated plates [17].

	Resonance	COMSOL frequency	EXPERIMENTAL frequency
Circular	1st	135 kHz	137 kHz
	2nd	257 kHz	260 kHz
	3rd	257 kHz	260 kHz
Elliptical	1st	106 kHz	93 kHz
	2nd	174 kHz	167 kHz
	3rd	228 kHz	230 kHz
	4th	262 kHz	258 kHz
Two thickness	1st	129 kHz	127 kHz
	2nd	209 kHz	202 kHz
	3rd	266 kHz	260 kHz
	4th	302 kHz	305 kHz

Lastly, the simulation is taken one step further without a corresponding 3D printed structure. To approximate the design to the real moth's tympanum, damping is added by considering air as a viscous gas instead of an ideal one, and a point mass is

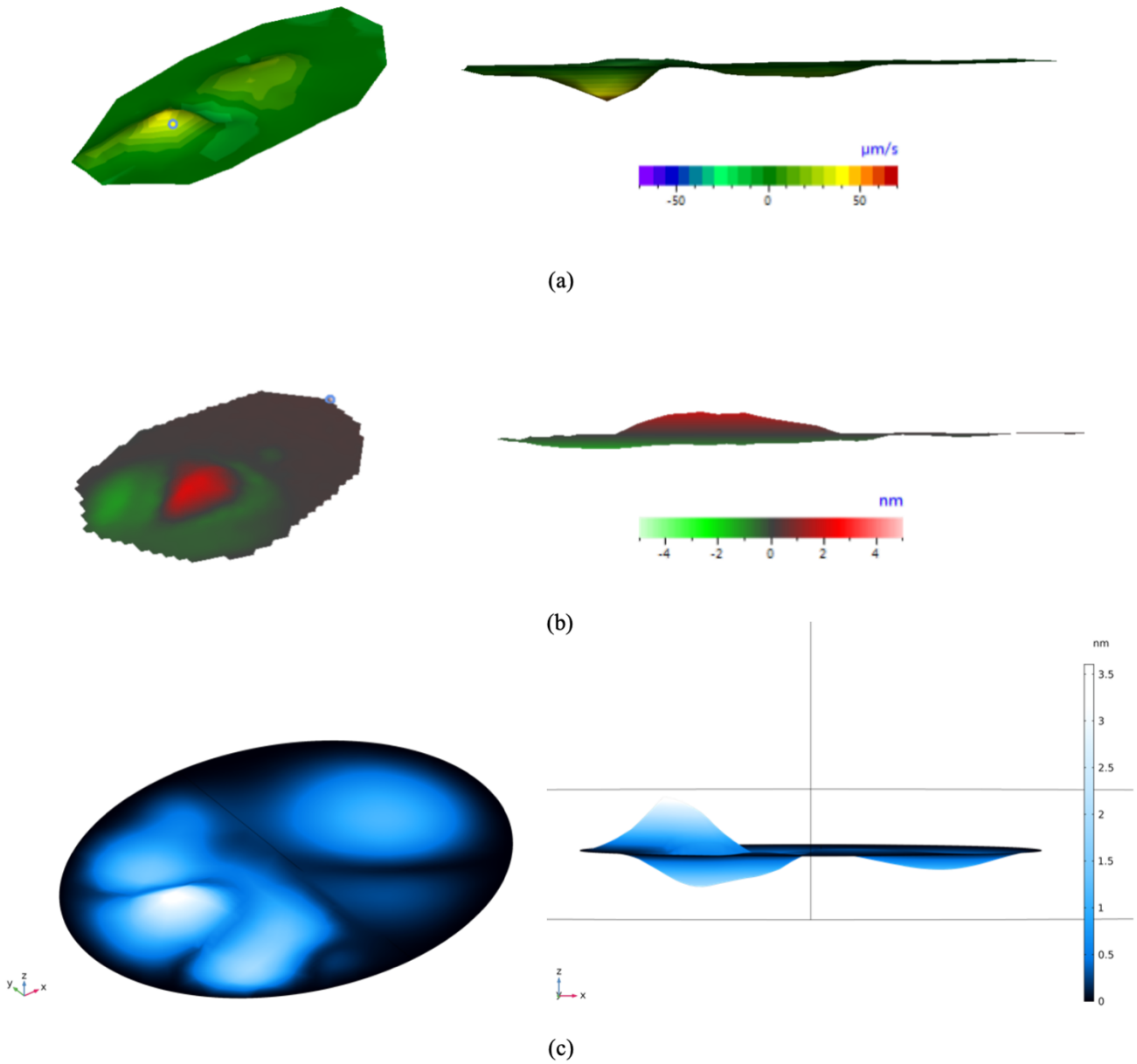

Fig. 4. (a) LDV measurement taken from a moth specimen showing the velocity at which the tympanum surface moves. (b) LDV measurement taken from a moth specimen showing displacement of the tympanum surface. (c) COMSOL simulation of the sixth natural frequency of an elliptical plate divided in two sections of different thicknesses (thin one on the left half of the ellipse and thick one on the right) with an attached mass (perspective view on the left and XZ plane view on the right).

added in the center of the thin section, to account for the neuron attachment. The mass chosen is one of an estimated biological relevance, equal to the mass of the whole plate but concentrated on one spot. Upon examination of the eigenfrequencies for this model, the sixth one (Fig. 4 c) is found to be quite an accurate reflection of the movement observed in the moth's tympanum, for which two scans can be seen in Fig. 4 a and b.

C. Directivity Response

Once the method was validated, the directionality response of the structures was measured. For this the piezoelectric chip cannot be used to excite the plates, since the stimulus must be acoustic, at a distance and allow the structure (or stimulus) to be rotated. For this reason, the structures used the custom resin and slightly altered design, as explained in the methods. In this part of the work, only the elliptical, two-thickness, plates are considered, which is the model that is expected to provide the most directionality from simulations. According to COMSOL, a switch in the directivity pattern is expected when exciting at the first and second resonant frequencies.

The piezoelectric chip was used initially to extract the frequency response of the plate printed with the new resin. A resulting spectrum is shown in Fig. 5. With the LDV software, the resonant frequencies are identified by comparison with the mode shapes produced by COMSOL. The first two are found to

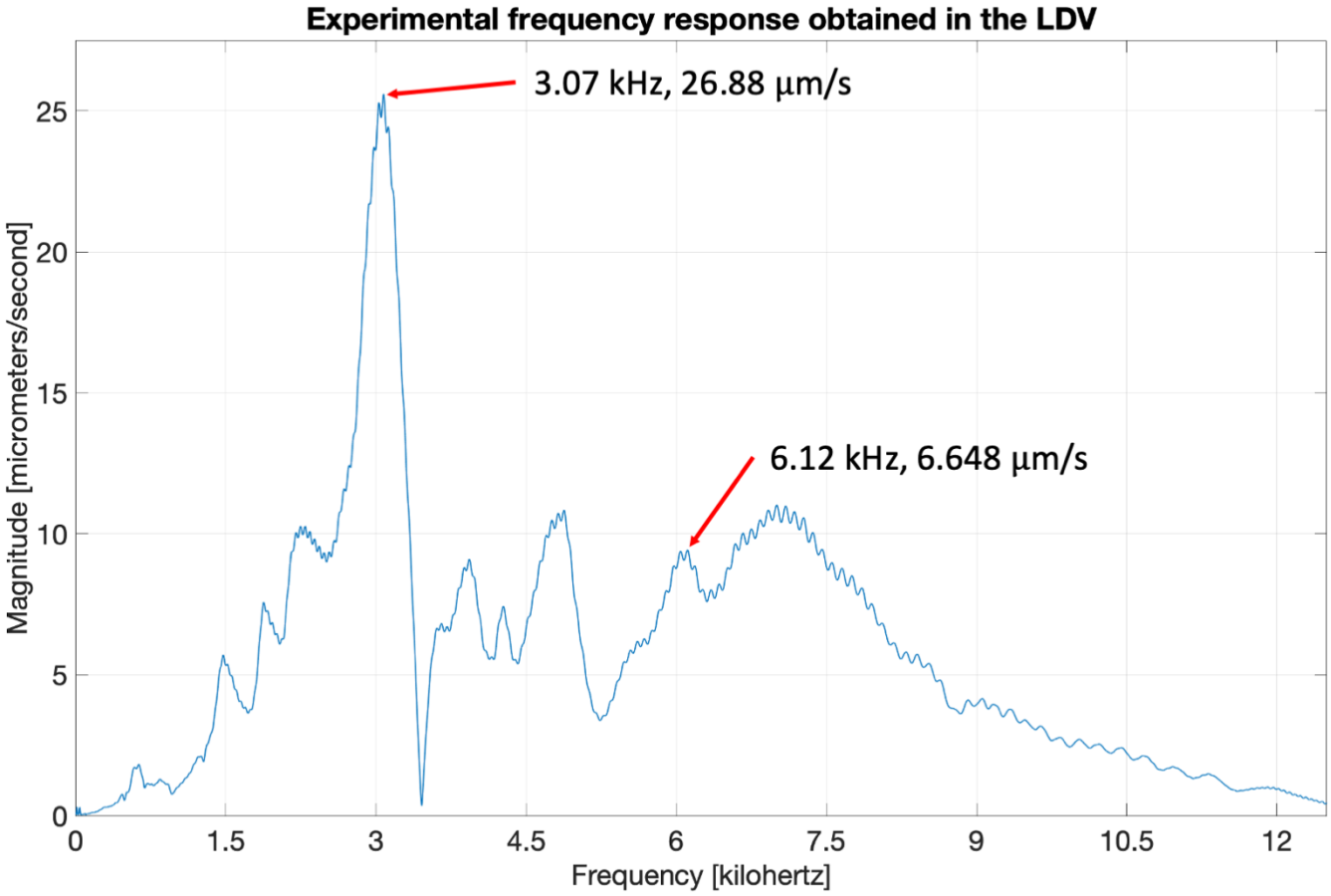

Fig. 5. Experimental frequency response of the custom resin two-thickness elliptical plate, obtained by excitation with the piezoelectric chip, with first and second resonances' location tagged.

be located at 3.074 kHz and 6.117 kHz respectively (tagged within the graph). COMSOL's prediction situates them at 4.6499 kHz and 7.053 kHz, such that both are slightly higher in frequency.

The resulting plots can be seen in Fig. 6 in a side-by-side comparison with the directivity plots produced by COMSOL. The shapes of the polar patterns are reasonably in agreement with the ideal version produced by COMSOL. In the case of the first resonant frequency (images a and b), a clear preference for the rear is seen; and in the case of the second frequency response (c and d), the preference seems to be towards the front, with a slight narrowing that results in a small lobe pointing towards the back, such as the one present in the COMSOL simulation.

IV. Conclusions

This work suggests that the morphology of the moth's tympanum can be replicated, and directivity is seen in simplified 3D printed versions of the system.

The discrepancy between experimental and simulated resonant frequencies for the printed structures can be at least partly attributed to the difficulties of the 3D printing process, as mentioned towards the end of section II. C. Irregularities on the surface of the plates can be seen in the LDV and a non-uniform thickness in the sections in the x-ray scans. There is also a source of human error in the process of locating the measuring point for the directionality measurements (there is a notch at the center of the thin section, but it must be located through the LDV vision system after each turn). A more trustworthy manufacturing process would palliate the irregularities of the surface, and a robotic automatization of the process of finding the measuring point or similar would also increase the precision. Nevertheless, the structures printed in this work reproduce the directivity patterns as expected from simulation results.

These promising results lead to future work including, but not limited to, adding a concentrated mass on the 3D printed plates to account for the moth's neuron attachment and taking the design forward to becoming an acoustic sensor by printing the model in piezoelectric materials to get an electric response when exposed to sound. Another path to explore is how to widen the sensitivity bandwidth of the plate, for it would be desirable to turn our system into a wideband sensor for applications like hearing aids.

Acknowledgment

The authors want to thank Lisa Asciak's help in mechanically testing the PEGDA samples to contrast the measurement of Young's modulus.

References

[1] D. Robert, 'Directional Hearing in Insects', in Sound Source Localization, A. N. Popper and R. R. Fay, Eds. New York, NY: Springer, 2005, pp. 6–35, doi: 10.1007/0-387-28863-5_2

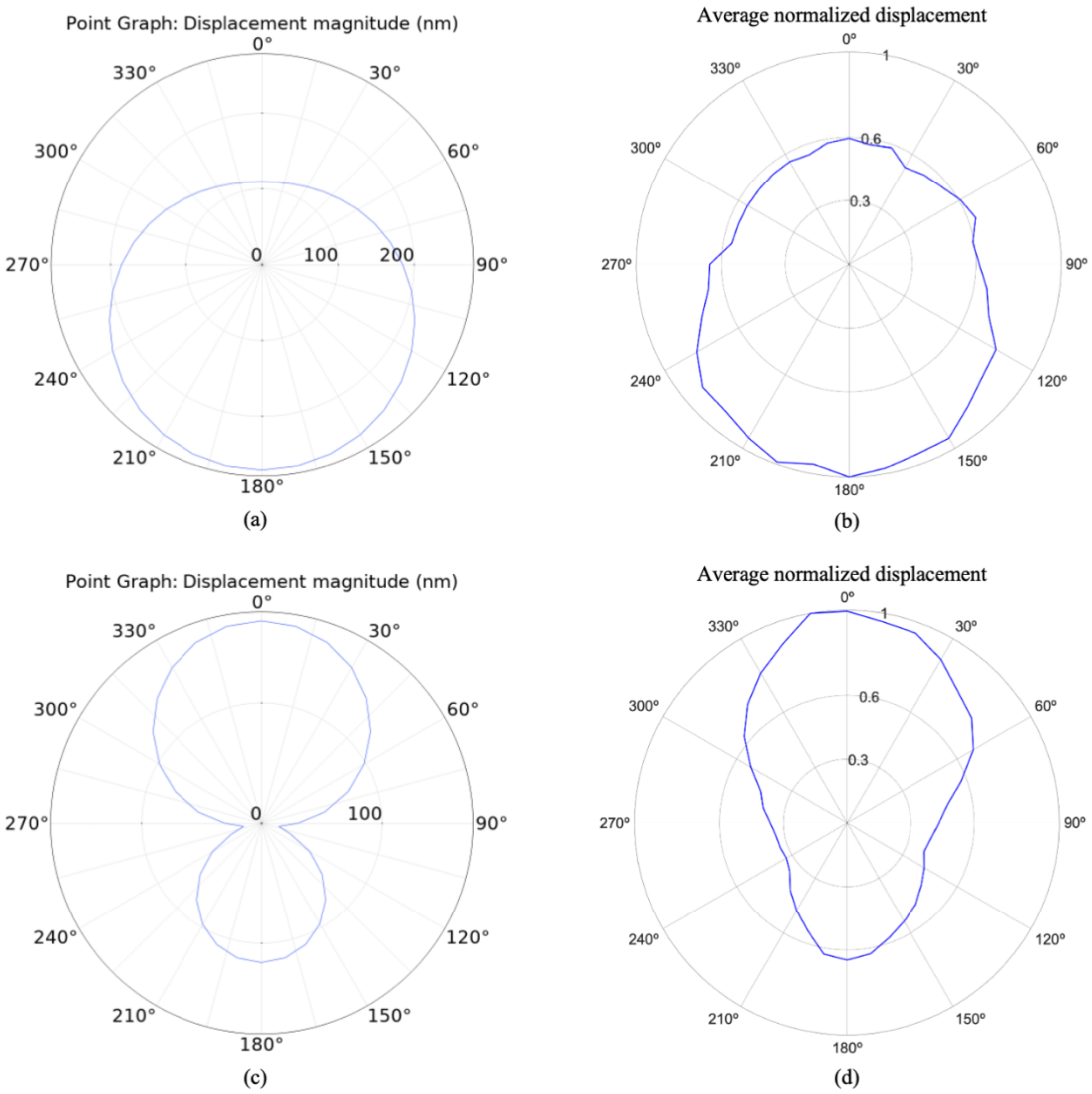

Fig. 6. COMSOL and experimental directivity plots for the two-thickness elliptical plate. Images a (simulated) and b (experimental) correspond to the first resonant frequency. Images c (simulated) and d (experimental) correspond to the second resonant frequency.

[2] R. S. Edgecomb, D. Robert, M. P. Read, and R. R. Hoy, 'The tympanal hearing organ of a fly: phylogenetic analysis of its morphological origins', Cell Tissue Res., vol. 282, no. 2, pp. 251–268, Nov. 1995, doi: 10.1007/BF00319116.

[3] R. N. Miles, D. Robert, and R. R. Hoy, 'Mechanically coupled ears for directional hearing in the parasitoid fly Ormia ochracea', J. Acoust. Soc. Am., vol. 98, no. 6, p. 3059, Jun. 1998, doi: 10.1121/1.413830.

[4] A. C. Mason, M. L. Oshinsky, and R. R. Hoy, 'Hyperacute directional hearing in a microscale auditory system', Nature, vol. 410, no. 6829, pp. 686–691, Apr. 2001, doi: 10.1038/35070564

[5] W. H. Cade, M. Ciceran, and A. M. Murray, 'Temporal patterns of parasitoid fly (Ormia ochracea) attraction to field cricket song (Gryllus integer)', Can. J. Zool., Feb. 2011, doi: 10.1139/z96-046.

[6] J. Schul, M. Holderied, D. Von Helversen, and O. Von Helversen, 'Directional hearing in grasshoppers: neurophysiological testing of a bioacoustic model', J. Exp. Biol., vol. 202, no. 2, p. 121, 1999, doi: 10.1242/jeb.202.2.121.

[7] A. Michelsen, A. V. Popov, and B. Lewis, 'Physics of directional hearing in the cricket Gryllus bimaculatus', J. Comp. Physiol. A, vol. 175, no. 2, pp. 153–164, Aug. 1994, doi: 10.1007/BF00215111.

[8] G. S. Pollack, A. C. Mason, A. N. Popper, and R. R. Fay, Insect hearing. Springer, 2016, doi: 10.1007/978-3-319-28890-1.

[9] M. D. Greenfield, 'Acoustic Communication in the Nocturnal Lepidoptera', in Insect Hearing and Acoustic Communication, B. Hedwig, Ed. Berlin, Heidelberg: Springer, 2014, pp. 81–100, doi: 10.1007/978-3-642-40462-7.

[10] J. L. Eaton, Lepidopteran anatomy. New York; Chichester; Brisbane: J. Wiley & Sons, 1988, doi: 10.1086/416282.

[11] L. Knopek and C. Hintze-Podufal, 'Uber den Bau der abdominalen Tympanalorgane der Kleinen Wachsmotte Achroia grisella (Fbr.)', Zool. Jahrbuecher Abt. Fuer Anat. Ontog. Tiere, vol. 1141, pp. 83–93, Jan. 1986.

[12] R. L. Rodríguez and M. D. Greenfield, 'Behavioural context regulates dual function of ultrasonic hearing in lesser waxmoths: bat avoidance and pair formation', Physiol. Entomol., vol. 29, no. 2, pp. 159–168, 2004, doi: 10.1111/j.1365-3032.2004.00380.x.

[13] A. Reid, T. Marin-Cudraz, J. F. Windmill, and M. D. Greenfield, 'Evolution of directional hearing in moths via conversion of bat detection devices to asymmetric pressure gradient receivers', Proc. Natl. Acad.

Sci., vol. 113, no. 48, pp. E7740–E7748, 2016, doi: 10.1073/pnas.1615691113.
[14] H. G. Spangler and C. L. Hippenmeyer, 'Binaural phonotaxis in the lesser wax moth, Achroia grisella (F.) (Lepidoptera: Pyralidae)', J. Insect Behav., vol. 1, no. 1, pp. 117–122, Jan. 1988, doi: 10.1007/BF01052508.
[15] J. F. V. Vincent and U. G. K. Wegst, 'Design and mechanical properties of insect cuticle', Arthropod Struct. Dev., vol. 33, no. 3, pp. 187–199, Jul. 2004, doi: 10.1016/j.asd.2004.05.006.
[16] A. Reid, 'Directional hearing at the micro-scale: bio-inspired sound localization', University of Strathclyde thesis, 2017, doi: 10.48730/7r6d-aq98.
[17] L. Díaz-García, A. Reid, J. Jackson and J. F. C. Windmill, "Towards a bio-inspired acoustic sensor: Achroia grisella's ear," 2021 IEEE Sensors, 2021, pp. 1-4, doi: 10.1109/SENSORS47087.2021.9639528.
[18] H. Gong, M. Beauchamp, S. Perry, A. T. Woolley, and G. P. Nordin, 'Optical approach to resin formulation for 3D printed microfluidics', RSC Adv., vol. 5, no. 129, pp. 106621–106632, 2015, doi: 10.1039/C5RA23855B.
[19] H. Mao et al., 'Twist, tilt and stretch: From isometric Kelvin cells to anisotropic cellular materials', Mater. Des., vol. 193, p. 108855, Aug. 2020, doi: 10.1016/j.matdes.2020.108855.
[20] B. Tiller et al., 'Piezoelectric microphone via a digital light processing 3D printing process', Mater. Des., vol. 165, p. 107593, Mar. 2019, doi: 10.1016/j.matdes.2019.107593.
[21] D. Wu, Z. Zhao, Q. Zhang, H. Jerry Qi, and D. Fang, 'Mechanics of shape distortion of DLP 3D printed structures during UV post-curing', Soft Matter, vol. 15, no. 30, pp. 6151–6159, 2019, doi: 10.1039/C9SM00725C.
[22] J. Wu et al., 'Evolution of material properties during free radical photopolymerization', J. Mech. Phys. Solids, vol. 112, pp. 25–49, Mar. 2018, doi: 10.1016/j.jmps.2017.11.018.
[23] P. S. Bychkov, V. M. Kozintsev, A. V. Manzhirov, and A. L. Popov, 'Determination of Residual Stresses in Products in Additive Production by the Layer-by-Layer Photopolymerization Method', Mech. Solids, vol. 52, no. 5, pp. 524–529, Sep. 2017, doi: 10.3103/S0025654417050077.
[24] A. Reid, J. C. Jackson, and J. F. C. Windmill, 'Voxel based method for predictive modelling of solidification and stress in digital light processing based additive manufacture', Soft Matter, vol. 17, no. 7, pp. 1881–1887, Feb. 2021, doi: 10.1039/D0SM01968B.
[25] J. M. Gere and S. P. Timoshenko, Mechanics of materials. Boston: PWS Publishing Company, 1997, doi: 10.1007/978-1-4899-3124-5.

Lara Díaz-García received her bachelor's degree in physics from Universidad de La Laguna in 2016 and her master's degree in acoustics and music technology from the University of Edinburgh in 2017. She is currently pursuing her PhD in the Centre for Ultrasonic Engineering in the University of Strathclyde. Her research interests are varied, from biologically inspired acoustic sensors to the acoustics of musical instruments.

Andrew Reid is a Leverhulme Fellow at the Centre for Ultrasonic Engineering at Strathclyde. He received a B.Eng in Electrical and Mechanical Engineering in 2012 and a PhD degree in insect inspired acoustics from the same institution in 2016. His research interests are in soft and flexible sensors and actuators, spanning novel manufacuring methods and 3D printing techniques to systems design.

Joseph C. Jackson-Camargo received the MSc (Hons.) degree in physics from Imperial College London, London, in 2003, and the Ph.D. degree in bio- logical sciences from the University of Bristol in 2008. He is currently a Lecturer in electrical and electronic engineering with the Centre for Ultrasonic Engineering, University of Strathclyde. His research interests cover a wide range of subjects, such as the physical basis for hearing, sound production and reception in biology and engineering, and advanced bio-inspired transducer and signal design.

James F. C. Windmill (M'99-SM'18) is a Professor in the Department of Electronic and Electrical Engineering, University of Strathclyde, Glasgow, U.K. He received a B.Eng. degree in electronic engineering from the University of Plymouth, UK, in 1998 and a Ph.D. degree in magnetic microscopy from University of Plymouth, UK, in 2002. He has over 20 years of research and development experience in the areas of sensors and hearing systems. His research interests are in the field of biologically inspired acoustic systems, from the fundamental biology to various engineering application topics.